Structural and Multidisciplinary Optimization (2022) 65:97
https://doi.org/10.1007/s00158-022-03178-0

RESEARCH PAPER

Exact global optimization of frame structures for additive manufacturing

Oguz Toragay[1] · Daniel F. Silva[1] · Alexander Vinel[1] · Nima Shamsaei[2]

Received: 4 June 2021 / Revised: 30 December 2021 / Accepted: 6 January 2022 / Published online: 28 February 2022

Abstract

We consider the problem of designing lightweight load-bearing frame structures with additive manufacturability constraints. Specifically, we focus on mathematical programming approaches to finding exact globally optimal solutions, given a pre-specified discrete ground structure and continuous design element dimensions. We take advantage of stiffness matrix decomposition techniques and expand on some of the existing modeling approaches, including exact mixed-integer nonlinear programming and its mixed-integer linear programming restrictions. We propose a (non-convex) quadratic formulation using semi-continuous variables, motivated by recent progress in state-of-the-art quadratic solvers, and demonstrate how some additive-specific restrictions can be incorporated into mathematical optimization. While we show with numerical experiments that the proposed methods significantly reduce the required solution time for finding global optima compared to other formulations, we also observe that even with these new techniques and advanced computational resources, discrete modeling of frame structures remains a tremendously challenging problem.

Keywords Discrete topology optimization · Additive manufacturing · Frame structures · Mixed integer non-linear programming · Mixed integer quadratically constrained programming · Mixed integer linear programming

Sets

$\mathbb{S}_{\text{dof}}$	Set of all degrees of freedom in the ground structure ($3 \times$ number of nodes)
$\mathbb{S}_{\text{e}}$	Set of all potential elements in ground structure
$\mathbb{S}_n$	Set of all nodes in the ground structure
$\mathcal{D}_{(k)}$	Set of all degrees of freedom on node k
$\mathcal{H}_{(k)}$	Set of elements in the neighbourhood of node k
$\mathcal{S}$	Set of all (e_1, e_2) pairs with $e_1, e_2 \in \mathbb{S}_e$ such that e_1 may intersects e_2

Parameters

$a_{\max}$	Upper bound on a_e variable
$a_{\min}$	Lower bound on a_e variable
$u_{\max}$	Upper bound on displacement on each DoF
l_e	Preliminary length of beam element e
$\mathcal{N}_{(e)}$	(n_1, n_2) pair of nodes with $n_1, n_2 \in \mathbb{S}_n$ such that element e connects n_1 and n_2
θ_e	Angle between element e and horizontal line
$\mathbf{k}_e$	Stiffness matrix of element e
$\mathbf{b}_{ei}$	Vectors to generate stiffness matrix for element e ($i \in \{1, 2, 3\}$)
$\mathbf{K}$	Structure's stiffness matrix
E	Young modulus of elasticity
d	Number of all degrees of freedom in the structure
p_j	External load on degree of freedom j
$\mathbf{P}$	Vector of all external nodal loads in the structure
ρ	Density of the used material

Design Variables

$\mathbf{a}$	Vector of all elements' cross-sectional area
a_e	Circular cross-sectional area of element e $\in \mathbb{R}^+$
x_e	Indicates the inclusion of beam element e in the resulted structure $\in \{0, 1\}$
x_{ec}	Indicates that profile c is chosen for element e in the resulted structure $\in \{0, 1\}$
y_k	Indicates the inclusion of node k in the resulted structure $\in \{0, 1\}$

Responsible Editor: Matthew Gilbert.

✉ Oguz Toragay
oguz@auburn.edu

[1] Industrial and Systems Engineering Department, Auburn University, Auburn, USA

[2] Mechanical Engineering Department, Auburn University, Auburn, USA

State Variables

I_e	Moment of inertia of element e	$\in \mathbb{R}$
$\mathbf{I}$	Vector of I_es for all elements	$\in \mathbb{R}^{\lvert\mathbb{S}_e\rvert\times 1}$
u_j	Displacement on degree of freedom j	$\in \mathbb{R}$
$\mathbf{u}$	Vector of displacements on all DoF	$\in \mathbb{R}^{d\times 1}$

1 Introduction

Design of lightweight structures is an important task for many engineering fields, including mechanical, civil, aerospace, and biomedical engineering. Recently this interest has intensified due to advances in metal-based additive manufacturing (AM), which can vastly expand the variety of possible designs, albeit while introducing its own set of limitations. In this work, we specifically focus on additively manufactured frame structures. In designing such structures, it is usually assumed that a fixed ground structure is first established, which defines the set of possible elements. The problem is then in selecting a subset of these elements and their dimensions, in a way that can be feasibly manufactured and such that the overall structure can withstand a pre-specified external load, while minimizing the structure weight (or vice versa, i.e., the structure that can withstand maximum load while satisfying a weight constraint). Figure 1 shows two examples of regular ground structures based on a grid, however, ground structures can assume any shape appropriate for the design task. The problem combines discrete (which elements are selected) and continuous (cross-sectional areas) decision variables, which is part of the reason why it can be computationally challenging. Recent advances in exact global optimization software and available computing resources suggest a potential for solving some of these instances to optimality. The goal of this study is to evaluate existing techniques and propose new ones that can take advantage of these advances, specifically in the context of AM.

Discrete structures can generally be classified into two types based on the mechanical behavior: trusses and frames. Trusses consist of pin-joined bar elements, i.e., elements that cannot convey bending moments while exposed to external loads. In contrast, frames are constructed from rigid-joint beams. On one hand, mechanical behavior of either type of structure is well-understood, and consequently, its response to any external load can be characterized numerically. On the other hand, optimizing the design can be an exceptionally challenging computational task for trusses and even more so for frames. As reviewed in Sect. 2, partially due to this computational challenge, truss structure optimization is relatively well-studied, whereas frame optimization is less common. By design, additively manufactured discrete structures are primarily modeled as frames, and consequently in this effort we focus on those.

The aim of this paper is to revisit the frame structure optimization problem over a given discrete ground structure. Specifically, we are interested in exact globally optimal solutions as opposed to heuristics. This is motivated by recent progress in capabilities of commercial global optimization solvers, particularly for non-convex quadratically constrained problems. Consequently, our specific research goals are as follows:

(A) Propose a mixed-integer quadratically constrained programming (MIQCP) formulation for minimum-weight frame structure with continuously measured beam-element cross-sectional area and restrictions on allowed displacements.
(B) Establish an approach to incorporate additive manufacturability constraints.
(C) Evaluate the potential for finding globally optimal structures using modern optimization solvers and available computational resources.

It is worth emphasizing here that while we do observe that the proposed MIQCP approach outperforms existing exact formulations and is better than or comparable to linear approximations (depending on the selection criterion and instance), the underlying problem remains computationally

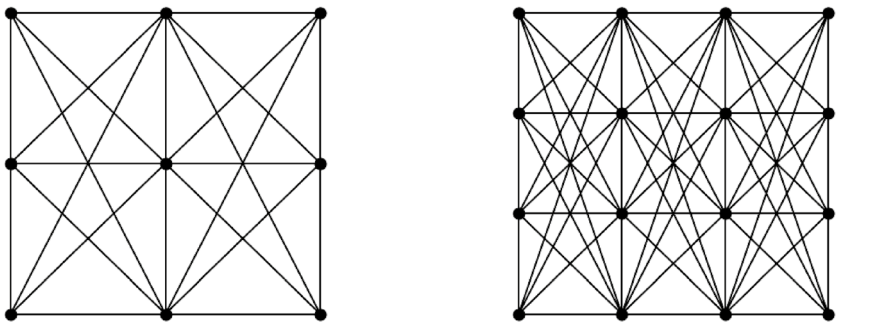

(a) 3×3 ground structure (b) 4×4 ground structure

Fig. 1 Examples of regular ground structures. Note that here all beams at angle less than 45° to the ground are excluded due to manufacturability restrictions

challenging. Therefore, in this research, we also set out to outline the scale of the problems that can be solved to global optimally. The results we present indicate that practical, realistically sized AM design problems still cannot be fully solved with exact methods. On the other hand, our findings can also inform the development of heuristic methods, more applicable for practical problems by serving as a subroutine or for validation.

The remainder of the paper is organized as follows. In Sect. 2 a review of related literature is given. After a brief explanation of the design problem, Sect. 3 presents three mathematical optimization models for solving the problem, two adapted from the literature and one proposed here. Each is supplemented with relevant AM constraints. Section 4 provides the results of the numerical experiments comparing the models. Section 5 concludes the paper by summarizing the main results and findings and providing a road map for future work. Finally, we show how the results of this work can be replicated.

2 Background

In this section, we first summarize relevant works in structural optimization (SO) in general and then narrow down our focus to lightweight frame structure fabrication by metal additive manufacturing, specifically. The concept of lightweight structures, or in other words, distribution of material in the most economical way, can be first attributed to Michell (1904). Since then, the topic has received significant attention. SO methods can be categorized as (Stolpe 2016): *size optimization*, *shape optimization* and *topology optimization*. Size optimization focuses on the cross-sectional area of all elements in the ground structure where none of the elements are allowed to vanish. On the other hand, shape optimization changes the shape of the structure by modifying the nodal coordinates, member lengths, and member presence in the optimized structure. Topology optimization is a combination of these two, where both presence and size of the elements can be modified during the optimization process. For more details see, for example, Querin et al. (2017), and Bendsoe and Sigmund (2013). In the remainder of this section we focus on the topology optimization literature, as applied to frame and truss structures only.

Two main streams of research efforts in topology optimization of structures, have been established in the literature by Dorn (1964) for discrete structure's topology and by Bendsoe and Sigmund (2013) for continuum structure's topology. Ground structures or design domain basis for optimization procedure are widely used approaches, where fixed nodal locations are connected with a set of possible candidate elements (bars or beams). On this ground structure, applied load(s), boundary conditions and specific design restrictions are assumed to be given. According to Bendsoe and Sigmund (2013), the design variables in this case are the size, the shape, and the connectivity of the structure (i.e., which elements are selected). A thorough review of the related literature can be found in Stolpe (2016) for discrete and in Eschenauer and Olhoff (2001), and Deaton and Grandhi (2014) for continuum structures. Stolpe (2016) categorized the approaches for modeling topology optimization problems using the ground structure method as follows:

- minimum compliance (maximum stiffness) problem with the constraint on the structure's volume,
- minimum weight problem with constraint on the compliance,
- minimum weight problem with constraints on the nodal displacements and element stresses.

Note though, that from the mathematical programming perspective, these can often be considered as equivalent representations of the same multi-objective problem.

Truss structures. Using bar elements and consequently optimizing trusses as a discrete structure is a popular problem in the literature. As noted by Grossmann et al. (2014) if each bar's cross-sectional area is considered as the design variable, then the resulting optimization problem can be classified as non-convex nonlinear programming (NLP). Further, due to particular manufacturing constraints, design variables are often also restricted to take discrete values, which gives rise to mixed-integer nonlinear programs (MINLP). A Mixed Integer Linear Programming reformulation of such problems with separable objective functions and bilinearities in the constraints is given by Grossmann et al. (2014). Several approaches for tackling the truss topology optimization problem have been considered; see for example Bollapragada et al. (2001); Stolpe and Svanberg (2003);

Stolpe (2004); Rasmussen and Stolpe (2008); Achtziger and Stolpe (2007); Cerveira et al. (2013). Various mathematical modeling approaches have been proposed for truss structures. For example, mathematical program with complementarity constraints (MPCC) by Kočvara and Outrata (2006), second order cone programming (SOCP) by Lobo et al. (1998), and meta-heuristic methods by Kaveh and Zolghadr (2014) are some other approaches to solve the discrete topology optimization problem for truss structures. As observed by Makrodimopoulos et al. (2010), the popularity of truss structures is due to the simplicity of designing and the ease of mathematically formulating these structures. At the same time, by design, truss structure modeling is not practical for additively manufactured parts, giving rise to renewed interest in frame structure optimization.

Frame structures. While similar in problem statement to trusses, frame structure optimization is generally considered to be significantly more challenging from both the modeling and computational perspectives. Specific difficulties include: larger number of required variables, more complicated finite element analysis equations and higher-dimension and more involved structure of the stiffness matrix. Traditionally, frames have been considered for optimization of steel building structures. Since these are generally only fabricated in discrete standard sizes, such frame optimization problems necessarily involve discrete design decision variables. Early approaches employed rounding of continuous variables, which can result in inferior results (Chan 1992). An extensive review of mathematical programming and meta-heuristic methods for optimization of frame structures is given by Saka and Geem (2013). Some notable examples include, Optimality Criteria method proposed by Chan (1992), Genetic Algorithm-based approach implemented by Erbatur et al. (2000), outer-approximation/equality-relaxation iterative algorithm proposed by Klanšek et al. (2007) and Karush-Kuhn-Tucker (KKT) conditions and the complementary strain energy method proposed by Takezawa et al. (2007). Other, more recent approaches include: mixed-integer second-order cone programming that Kanno (2016) proposed, robust optimization, and gradient-based optimization proposed by Changizi and Jalalpour (2017a, 2017b), and even a combination of reinforcement learning (RL) and meta-heuristics proposed by Hayashi and Ohsaki (2020). An important tool for improving computational tractability of the underlying mathematical programming problem, which we also employ in this effort, is decomposition of the stiffness matrix. In a series of papers (Stolpe and Svanberg 2003; Rasmussen and Stolpe 2008; Stolpe 2007) this approach was developed for trusses and then extended to frame structures. Kureta and Kanno (2014) implemented similar approach when considering the design of periodic frame structures with negative Poisson's ratio. We elaborate on the details of in Sect. 3 as it is related to the method proposed here.

Applications to additive manufacturing. AM methods have led to a radical change in the way that design for fabrication problems are considered, which includes new frontiers for topology optimization. Two particularly relevant reviews are given by Wang et al. (2016) and Liu and Ma (2016). The former concentrates on existing approaches to using topology optimization for continuum material in medical implants specifically. The latter discusses additive manufacturing oriented topology optimization in general. For example, Cansizoglu et al. (2008) used electron beam melting (EBM) to fabricate 3D optimized frame structures. The design variable were joints' locations and the objective function was the compliance of the structure. They implemented Quasi-Newton line search for unconstrained optimization and sequential quadratic programming (SQP) for the models with constraints on the mechanical properties of the structure. They mentioned as a result that, they found "discrepancies between the performance of the theoretical structures and the physical EBM structures due to the layered fabrication approach". Smith et al. (2016) proposed a work-flow to start the design process from a design domain (which is not a ground structure due to continuity) by finding an optimized layout for the structure. Throughout a set of post-optimization steps, the resulting layout is converted to a continuum structure viable for additive manufacturing. To the best of our knowledge, there are only a few works focused on the applications of additive manufacturing in the fabrication of optimized discrete structures in comparison to the continuum structures. See for example Gorguluarslan et al. (2017), and Li and Chen (2010). Most of the applications in the literature focused on the continuum structures when the material distribution among design area is optimized by removing the material that is less desired (making holes in the continuum design domain). This is due mainly to the fact that discrete frame structure optimization problems remain extremely challenging computationally, especially if exact global optimization is concerned. At the same time, recent progress in both availability of computational resources and quality of state-of-the-art non-convex global solver (particularly, the release of Gurobi solver for non-convex MIQCP problems), could expand potential applicability of discrete frame optimization.

The contribution of this paper is two-fold. First, we propose a mixed-integer quadratically constrained programming formulation for frame structure optimization problem, while taking into account additive manufacturability constraints. The formulation is equivalent to the exact optimization

problem (unlike linear reformulation), and as such is guaranteed to achieve global optimum (given enough computational resources), and is designed to take advantage of modern advances in optimization solvers. Second, we evaluate the potential for finding globally optimal solutions for frame structure design problems as a problem class, in light of the aforementioned advances in solver technology, as well as computational resources. While we are able to demonstrate that the proposed MIQCP formulation performs well compared to other existing models (specifically, outperforms the naive nonlinear model across the board, and is better or comparable with MILP restricted formulations), we also observe that despite these efforts, only a very limited set of instances can actually be solved to global optimality in a reasonable time.

3 Mathematical models

We consider three modeling approaches to the frame structures optimization problem, referred to as: mixed integer non-linear programming (`MINLP`), mixed integer quadratically constrained programming (`MIQCP`) and mixed integer linear programming (`MILP`) models. `MINLP` and `MILP` models are adapted from the literature with additional improvements and modifications that enable these models to allow for additive manufacturability constraints. The proposed `MIQCP` model is novel to this work. In it we use semi-continuous variables for defining the beam elements' cross-sectional areas, which allows for reformulating the general non-linear constraints as quadratic.

3.1 General problem statement and stiffness matrix decomposition

We consider the following general form of the weight minimization problem for a frame structure:

minimize weight of the structure

subject to $\mathbf{K}(\mathbf{a}, \mathbf{I})\mathbf{u} = \mathbf{P}$

$u_{\min} \leq \mathbf{u} \leq u_{\max}$

manufacturability constraints,

where it is assumed that a planar ground structure is given (sets $\mathbb{S}_n$ and $\mathbb{S}_e$ of potential nodes and beams) and the candidate solution is defined by vector $\mathbf{a}$ of cross-sectional areas for each potential beam. Then the first constraint (equilibrium equations) allows for evaluation of node displacements, which can then be bounded in order to enforce overall mechanical response of the structure under a given load vector $\mathbf{P}$. Note that we could alternatively consider a formulation that minimizes displacements subject to a constraint on the total weight. The problem also requires manufacturability constraints, which can be specific to the additive manufacturing process. As the displacements are assumed to be small, Euler-Bernoulli beam elements can be used in analyzing the mechanical behavior and characteristics of the structure. We generate the ground structure based on the given length, width and number of nodes in each dimension of the target structure. Each node in the structure corresponds to 3 degrees of freedom (displacements in x and y directions and the rotational displacement). Hence, each beam element corresponds to 6 degrees of freedom. Compared to truss structures, where elements are not rigidly connected (and hence do not generate displacements due to rotation), frame structures result in a significantly more complicated stiffness matrix. In the case of trusses, stiffness matrix can be reformulated in such a way as to allow for naturally eliminating all non-linearity from the problem, which is generally impossible for frames. As an alternative to linearization, each 6×6 element of the stiffness matrix can be decomposed following an approach in Stolpe and Svanberg (2003); Stolpe (2004); Rasmussen and Stolpe (2008); Kanno (2016). A detailed description of the mechanical relations used in the decomposition is given in Appendix . This approach results in the following equation for the stiffness matrix $\mathbf{K}$:

$$\mathbf{K} = \sum_{e \in \mathbb{S}_e} a_e k_{e1} \mathbf{b_{e1}} \left(\mathbf{b_{e1}^\top}\right) + a_e^2 k_{e2} \mathbf{b_{e2}} \left(\mathbf{b_{e2}^\top}\right) + a_e^2 k_{e3} \mathbf{b_{e3}} \left(\mathbf{b_{e3}^\top}\right). \tag{3.1}$$

where constant values k_{ei} for each element e are defined as:

$$k_{e1} = \frac{E}{l_e}, \qquad k_{e2} = \frac{3E}{4\pi l_e}, \qquad k_{e3} = \frac{E}{4\pi l_e} \tag{3.2}$$

and $\mathbf{b_{ei}}$ is given by

$$\mathbf{b_{ei}} = \mathbf{T}_e^\top \times \mathbf{Trans}_e^\top \times \hat{\boldsymbol{b}}_{\boldsymbol{ei}}. \tag{3.3}$$

Note that in the equations above, $\mathbf{b_{ei}} \in \mathbb{R}^{d \times 1}$ are $d \times 1$ vectors from which the stiffness matrix $\mathbf{K} \in \mathbb{R}^{d \times d}$ can be generated. For the definitions of the matrices $\mathbf{T}_e^\top$, $\mathbf{Trans}_e^\top$, and $\hat{\boldsymbol{b}}_{\boldsymbol{ei}}$ that are used in the equation (3.3) we refer the reader to the Appendix. While it still results in a nonlinear expression, this decomposition is instrumental in allowing for formulating the models presented next.

3.2 Mixed integer non-linear programming model (`MINLP`)

The following `MINLP` formulation is obtained by directly applying the stiffness matrix decomposition to the general formulation, as well as enforcing AM manufacturability constraints. It serves as the basis for the other two formulations.

$$\textit{minimize}\ \ W_N = \sum_{e\in\mathbb{S}_e} \rho a_e l_e \qquad \text{(MINLP00)}$$

subject to

$$\left(\sum_{e\in\mathbb{S}_e} a_e k_{e1}\mathbf{b_{e1}}(\mathbf{b_{e1}^\top}) + a_e^2 k_{e2}\mathbf{b_{e2}}(\mathbf{b_{e2}^\top}) + a_e^2 k_{e3}\mathbf{b_{e3}}(\mathbf{b_{e3}^\top})\right)_i \mathbf{u} = p_i \qquad \forall i \in \mathbb{S}_{\text{dof}} \qquad \text{(MINLP01)}$$

$$-y_k u_{\max} \le u_j \le y_k u_{\max} \qquad \forall k \in \mathbb{S}_n \quad \forall j \in \mathcal{D}_{(k)} \qquad \text{(MINLP02)}$$

$$a_{\min} x_e \le a_e \le a_{\max} x_e \qquad \forall e \in \mathbb{S}_e \qquad \text{(MINLP03)}$$

$$x_{e_1} + x_{e_2} \le 1 \qquad \forall (e_1, e_2) \in \mathcal{S} \qquad \text{(MINLP04)}$$

$$2y_k \le \sum_e x_e \qquad \forall k \in \mathbb{S}_n \quad \forall e \in \mathcal{H}_{(k)} \qquad \text{(MINLP05)}$$

$$2x_e \le y_{n_1} + y_{n_2} \qquad \forall e \in \mathbb{S}_e \quad (n_1, n_2) \in \mathcal{N}_{(e)} \qquad \text{(MINLP06)}$$

$$x_e \in \{0, 1\} \qquad \forall e \in \mathbb{S}_e \qquad \text{(MINLP07)}$$

$$y_k \in \{0, 1\} \qquad \forall k \in \mathbb{S}_n \qquad \text{(MINLP08)}$$

$$a_e \ge 0 \qquad \forall e \in \mathbb{S}_e \qquad \text{(MINLP09)}$$

$$u_j \in \mathbb{R} \qquad \forall j \in \mathbb{S}_{\text{dof}} \qquad \text{(MINLP10)}$$

The variables can be split into two categories. *Decision variables* are the independent quantities related to element placement and their cross-sectional areas, while *state variables* are the dependent values determining the response to the external load given the specified structure, i.e., the internal forces, displacements, etc. Note that fixing the decision variables, fully determines the state variables (albeit, through nonlinear equations). The objective function (MINLP00), denoted as W_N, gives the total weight of the structure where ρ is the material density. Constraint (MINLP01) enforces the equilibrium equations by employing the stiffness matrix decomposition discussed above. Note that by decomposing the stiffness matrix it is possible to separate the variable portion from the fixed portion in the matrix. To limit the deformation of the structure under the external load, we bound the displacement on each degree of freedom to be in a predefined range in constraint (MINLP02). In this constraint, without loss of generality we assume that $u_{\min} = -u_{\max}$. To account for the fact that displacement on any nodes can be non-zero if and only if the node is connected to the resulting structure by at least one element we define a binary variable y_k for each node k in the ground structure to indicate the connectivity of node k to the body of the resulting structure.

The rest of the constraints explicitly account for some of the AM-related limitations. First, in addition to the upper bound on the cross-sectional area ($a_{\max}$), a lower bound must be enforced, due to the laser and powder interactions. Note though that the lower bound is only applicable to the beams that are present in the structure. Consequently, we define a binary variable, x_e, referring to whether beam e is included. Constraint (MINLP03) enforces the cross-sectional area bounds. Note that this constraint also eliminates the possibility of an element present in the structure with zero cross-sectional area.

Unlike truss structures, in planar frame structures, where the connections are fixed or welded (rigid joints), it is not desired (or even feasible) to have intersecting elements. If two elements intersect, they can no longer be correctly described in the balancing equations as two elements, and instead, should be replaced with four beams and an additional node (at the intersection point), which results in a different set of displacements. Hence a structure that allows for intersecting elements cannot be optimized with a fixed ground structure, and either needs to exclude such elements, or allow for creation of new nodes and elements. Methods following the latter approach are possible, see for example Cui et al. (2018) for the case of truss structures. However, this approach can lead to very long solution times, as the process is iterative and node addition can go on (in theory) indefinitely. Consequently, such a method may not be able to guarantee global optimality, even in theory. Due to the inherent difficulty of solving frame structures, we choose a different approach, by explicitly excluding intersecting elements. To this end, constraint (MINLP04) eliminates those intersections, by listing all pairs of beams that cannot be simultaneously included in the structure.

Finally, constraint (MINLP05) makes sure that the problem does not contain any "hanging elements", which here are defined as nodes with only single beam attached (with

the exception of fixed boundary nodes and external load locations). Note that, "hanging elements", cannot be present in a globally optimal solution by definition (as these add weight and do not contribute to supporting the load), and hence, this constraint is not necessary. On the other hand, we have observed that it improves the solution time, by excluding certain subregions of the feasible set that are known to not contain the optimal solution.

Another manufacturability restriction can be accounted for directly in the definition of the ground structure itself. Specifically, AM process requires that unless the structure is able to support itself (i.e., the angle between any beam and the ground is more than a certain threshold), additional support structures should be employed to avoid warping, see for example, Liu and Yu (2020). These can be undesirable, since, if used, they increase the material (metal powder) consumption and require specialized post-processing, which may not be feasible for all geometries/designs (Wang et al. 2019). To avoid this we can exclude all low-angle elements from the ground structure. It must be emphasized that, as defined, this approach is general, in the sense that any specific criterion for including/excluding elements in the ground structure can be accommodated. Further, since this is done before model formulation step (and before solution step), the three modeling approaches discussed in the this section are compatible with any ground structure and do not depend on the specific choice of the manufacturability angle criterion. For illustration purposes, in all examples and numerical experiments below we assume the low-angle threshold of 45° without loss of generality following Wang et al. (2013), while allowing for strictly horizontal beams (Liu and Yu 2020). Naturally, the models can be constructed for any other value of the angle analogously.

Overall, the problem given is then a mixed-integer non-convex nonlinear programming problem (here, the non-convex property refers to the non-convex continuous relaxation rather than the non-convexity due to integer variables), which cannot be linearized without loss of generality. One possible approach, discussed in the following section, is to restrict the continuous cross-sectional areas to only a discrete set of values, in which case linearization is possible.

3.3 Mixed integer linear programming model (MILP)

As noted earlier, in a traditional setting, the primary reason for discretizing potential cross-sectional areas (or diameters) of the structural elements in topology optimization was the fact that these elements were usually manufactured and available in pre-defined standard cross-sectional sizes and shapes. AM naturally relaxes this requirement, allowing for continuous decision variables.

Though, if discretization is applied, then it is possible to linearize the formulation above. Naturally, the resulting problem is not equivalent to the MINLP formulation, as it restricts the potential solutions. Note also that the linearization described below relies on introducing additional binary variables, and hence, it is not clear whether the computational benefit of relaxing nonlinear constraints outweighs the burden due to the extra variables.

The model in this section is similar to the linear model proposed by Kureta and Kanno (2014). We modify it in order to be able to compare the results to the nonlinear models. We define the discrete cross-sectional area candidate set as $C = \{0, c_1, c_2, ..., c_{pr}\}$. In general, this set can be element-specific without changing the structure of the model. Value pr gives the number of different non-zero discrete cross-sectional area profiles that we defined in the set C ($|C| = pr + 1$). For each element $e \in \mathbb{S}_e$ and each $c \in C$, we also define a profile which includes the cross-sectional area of the element (a_{ec}), moment of inertia I_{ec} (calculated using A.2) and length of the element (l_e). We can then define binary variable:

$$x_{ec} = \begin{cases} 1 & \text{if profile } c \text{ is chosen for element } e \\ 0 & \text{otherwise.} \end{cases} \tag{3.5}$$

For this formulation a_{ec} is a parameter defined as cross-sectional area of the selected profile c for element e. Consequently, we can linearize all constraints with the usual "big-M" method.

$$\textit{minimize}\ \ W_L = \sum_{e\in\mathbb{S}_e} \rho l_e \sum_{c\in C} a_{ec}x_{ec} \qquad \text{(MILP00)}$$

subject to

$$\sum_{e\in\mathbb{S}_e}\sum_{c=0}^{pr+1} a_{ec}k_{e1}v_{ec1}\mathbf{b_{e1}}(i) + a_{ec}^2k_{e2}v_{ec2}\mathbf{b_{e2}}(i) + a_{ec}^2k_{e3}v_{ec3}\mathbf{b_{e3}}(i) = p_i \qquad \forall i \in \mathbb{S}_{\text{dof}} \qquad \text{(MILP01)}$$

$$-M\left(1-\sum_{c=1}^{pr+1} x_{ec}\right) \le \sum_{c=1}^{pr+1} v_{ecj} - \mathbf{b_{ej}^\top u} \le M\left(1-\sum_{c=1}^{pr+1} x_{ec}\right) \qquad \forall e \in \mathbb{S}_e \quad j \in \{1,2,3\} \qquad \text{(MILP02)}$$

$$-M\left(\sum_{c=1}^{pr+1} x_{ec}\right) \le \sum_{c=1}^{pr+1} v_{ecj} \le M\left(\sum_{c=1}^{pr+1} x_{ec}\right) \qquad \forall e \in \mathbb{S}_e \qquad \text{(MILP03)}$$

$$\sum_{c\in C} x_{ec} = 1 \qquad \forall e \in \mathbb{S}_e \qquad \text{(MILP04)}$$

$$\sum_{c=1}^{pr+1} x_{ec} \le \tfrac{1}{2}\left(y_{n_1} + y_{n_2}\right) \qquad \forall e \in \mathbb{S}_e(n_1,n_2) \in \mathcal{N}_{(e)} \qquad \text{(MILP05)}$$

$$-y_k u_{\max} \le u_j \le y_k u_{\max} \qquad \forall k \in \mathbb{S}_n \quad \forall j \in \mathcal{D}_{(k)} \qquad \text{(MILP06)}$$

$$x_{e_1} + x_{e_2} \le 1 \qquad \forall (e_1,e_2) \in \mathcal{S} \qquad \text{(MILP07)}$$

$$2y_k \le \sum_e \sum_{c=1}^{pr+1} x_{ec} \qquad \forall k \in \mathbb{S}_n \quad \forall e \in \mathcal{H}_{(k)} \qquad \text{(MILP08)}$$

$$x_{ec} \in \{0,1\} \qquad \forall e \in \mathbb{S}_e \quad \forall c \in C \qquad \text{(MILP09)}$$

$$y_k \in \{0,1\} \qquad \forall k \in \mathbb{S}_n \qquad \text{(MILP10)}$$

$$v_{ecj} \in \mathbb{R} \qquad \forall e,c,j \qquad \text{(MILP11)}$$

Here we define a new variable v_{ecj} as the elongation of element e with profile c in direction j, where $j \in \{1,2,3\}$ representing horizontal (x), vertical (y), and rotational directions respectively. The presented formulation modifies constraint (MILP01) and adds constraints (MILP02), (MILP03) and (MILP04).

Constraint (MILP01) reformulates the equilibrium equation in the linear form. Constraint (MILP02) ensures that $v_{ecj} = \mathbf{b_{ej}^\top u}$ if element e is present in the structure. Constraint (MILP03) restricts the elongation of each element that is not set to 0. Finally, constraint (MILP04) forces exactly one profile from set C to be selected for element e. The rest of the constraints are directly analogous to the MINLP model.

3.4 Mixed integer quadratically constrained programming model (MIQCP)

Finally, we consider a modification of the MINLP model, that allows us to reformulate it as a mixed-integer (non-convex) quadratically constrained optimization problem. To the best of our knowledge this formulation, and this kind of model, has not been considered in the literature before for this problem.

Recall that a semi-continuous variable is a special kind of variable in a mathematical program, that is restricted to either zero or a continuous value from a pre-specified interval (which does not include zero). In our case, it naturally lends itself to representing cross-sectional areas, since those are restricted to be either zero or between $a_{\min}$ and $a_{\max}$ pre-defined cross-sectional area bounds. While in general a semi-continuous variable can be replaced with a pair of a binary and a continuous variable and a "big-M" constraint, some modern optimization solvers allow for direct modeling with such variables. This fact, in addition to the recent progress in non-convex quadratically constrained optimization, motivates the MIQCP formulation below. Note that using semi-continuous variables for cross-sectional areas eliminates the need for binary variables x_e used in MINLP formulation.

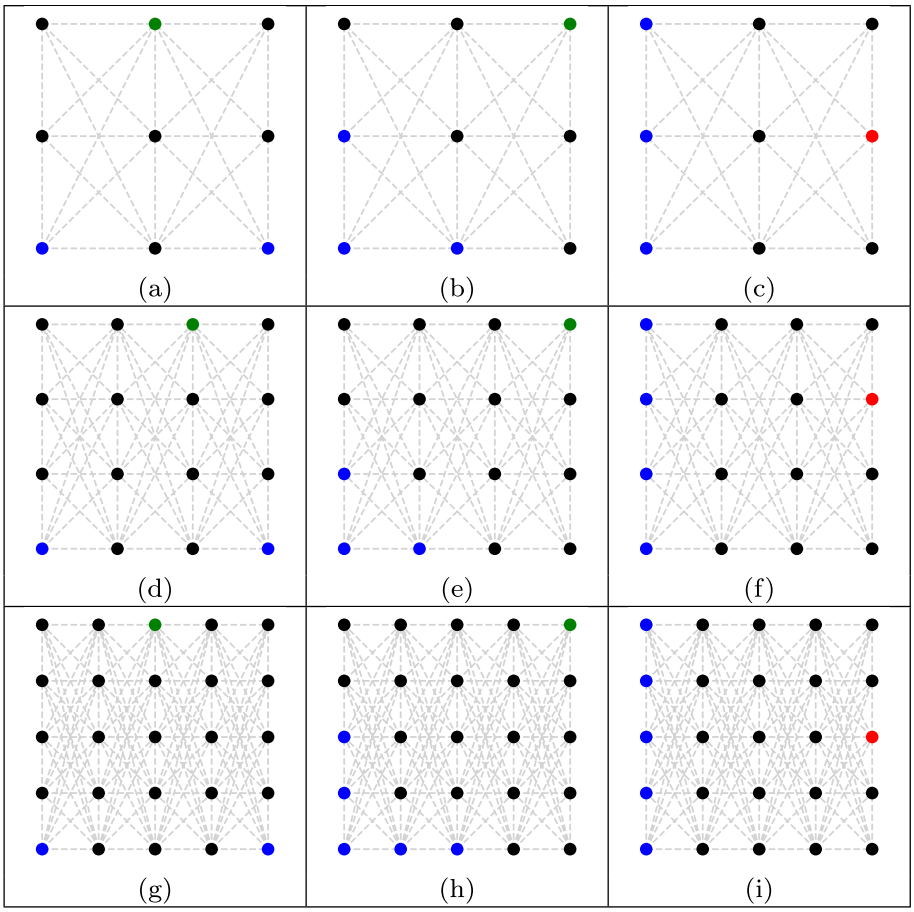

Fig. 2 Ground structures used in the experiments. Blue nodes represent the fixed nodes, while vertical upward and downward loads are applied at the green and red nodes respectively

$minimize\ \ W_Q = \sum_{e\in\mathbb{S}_e} \rho a_e l_e$		(MIQCP00)
subject to		
$\left(\sum_{e\in\mathbb{S}_e} a_e k_{e1}\mathbf{b_{e1}}(\mathbf{b_{e1}^\top}) + z_e k_{e2}\mathbf{b_{e2}}(\mathbf{b_{e2}^\top}) + z_e k_{e3}\mathbf{b_{e3}}(\mathbf{b_{e3}^\top})\right)_i \mathbf{u} = p_i$	$\forall i \in \mathbb{S}_{\text{dof}}$	(MIQCP01)
$z_e = a_e^2$	$\forall e \in \mathbb{S}_e$	(MIQCP02)
$-M\left(\sum_e a_e\right) \le u_j \le M\left(\sum_e a_e\right)$	$\forall j \in \{j \in \mathbb{S}_{\text{dof}} \mid j \in \mathcal{D}_{(k)}, \forall e \in \mathcal{H}_{(k)}\}$	(MIQCP03)
$-u_{\max} \le u_j \le u_{\max}$	$\forall j \in \mathbb{S}_{\text{dof}}$	MIQCP04
$a_{e_1} a_{e_2} = 0$	$\forall (e_1, e_2) \in \mathcal{S}$	(MIQCP05)
$a_e \le y_{n_1} y_{n_2} a_{\max}$	$\forall (n_1, n_2) \in \mathcal{N}_{(e)}$	(MIQCP06)
$2y_k a_{\min} \le \sum_e a_e$	$\forall k \in \mathbb{S}_n \quad \forall e \in \mathcal{H}_{(k)}$	(MIQCP07)
$a_e \in \{0\} \cup [a_{\min}, a_{\max}]$	$\forall e \in \mathbb{S}_e$	(MIQCP08)
$z_e \in \{0\} \cup [a_{\min}^2, a_{\max}^2]$	$\forall e \in \mathbb{S}_e$	(MIQCP09)
$u_j \in \mathbb{R}$	$\forall j \in \mathbb{S}_{\text{dof}}$	(MIQCP10)

To preserve the quadratic structure of the constraints, we also introduce an auxiliary variable z_e, which is set to the square of a_e by constraint (MIQCP02). With these, it is now possible to reformulate the problem as a MIQCP. Compared to the MINLP formulation, some of the constraints have to be updated to eliminate variables x_e. Specifically, constraint (MIQCP03) enforces the limits on the displacements with a "big-M" technique, constraint (MIQCP05) removes intersecting beams, constraint (MIQCP06) ensures that both ends of an existing beam are included in the structure, and constraint (MIQCP07) eliminates hanging beams.

3.5 Solution approach

Most optimization algorithms benefit from either a warm-start or a quality initial solution, and consequently we also propose a simple numerical procedure aimed at providing those for the model in question. Specifically, we consider a two-stage framework, where in the first stage we solve the simplest possible version of the model: linear formulation with just one non-zero profile, which can be expected to be relatively computationally inexpensive; then feed the resulting feasible solution (a valid upper bound) to the three considered formulations. Specifically, in stage one, we define $C = \{0, c_{\max}\}$ and solve problem (MILP00)–(MILP11). It is guaranteed that: 1) if this problem is infeasible, then the underlying design problem is infeasible; 2) the obtained optimal solution is feasible to both MINLP and MIQCP and any version of MILP with $\{0, c_{\max}\} \subset C$. This implies that the resulting optimal solution can be provided as the incumbent to any of the three formulations. In terms of MIQCPs the advantage of the two-stage approach is two-fold. First, in some cases it speeds up the solution process. Second, without two-stage approach, MIQCP method is unable to find any feasible solution to most challenging problems, which, naturally, can be a significant drawback. Also note that since MIQCP formulation does not directly include variables x_{ij}, it needs to be amended accordingly.

4 Numerical experiments

4.1 Test instances

A problem instance is defined by: the ground structure (number and position of nodes), external loads/boundary conditions (locations and magnitude), material properties and the set C of cross-sectional area candidates (MILP model only). Next, we briefly describe each component separately.

Ground structures. Observe that, as defined, the problem allows for ground structures of any shape or form. At the same time, in this case study, for the sake of streamlining the discussion, we only consider regular structures defined as 3×3 (with 9 nodes and 24 elements), 4×4 (with 16 nodes and 60 elements), and 5×5 (with 25 nodes and 120 elements) grids. We assume 50 mm $\times$ 50 mm design domain (with proportionally adjusted inter-nodal distance). The ground structures (along with external loads discussed below) are depicted on Fig. 2.

As discussed in Sect. 3.2, all potential beams at angle less than 45° to the ground are excluded due to manufacturability restrictions with the exception of horizontal elements. It is worth emphasizing here that our methodology, as proposed, is general and allows for flexibility in customizing the specific definition of manufacturability that a designer prefers. While beam angle to the ground is a primary determinant of the ability to manufacture a beam without support, the exact value of feasible angles can depend on a number of factors, including, for example, material used or surface roughness tolerance. For a detailed discussion of the related factors, see for example, Liu and Yu (2020). For the purposes of demonstrating the capabilities of our methodology, in the case study and all examples used we assume that beams at angle less than 45° to the ground are not allowed. At the same time, in this study we do allow for horizontal beams, which, as discussed in Liu and Yu (2020), represent a special case. Other criteria for including or excluding beams to/from ground structure can be straightforwardly applied in a particular application by updating the ground structure

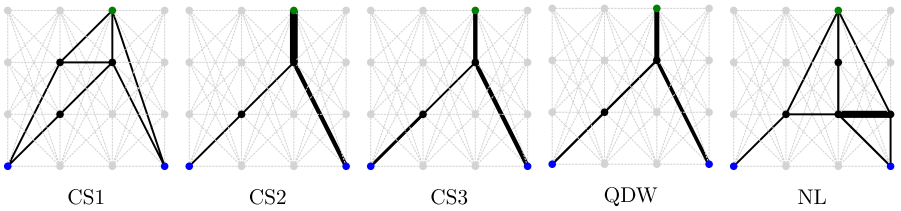

Fig. 3 Optimal structures found by five models for the instance based on ground structure (d) with 50 kN load. Beam widths are scaled for better viewing

Table 1 Weight of the best structures found by the 6 models

Structures from Fig. 2										
Load	Model	(a)	(b)	(c)	(d)	(e)	(f)	(g)	(h)	(i)
25	CS1	14.05	70.18	77.18	12.70	106.15*	79.21*	14.05	50.03*	81.88*
	CS2	14.05	38.10	59.63	12.70	84.10*	69.05*	14.05*	43.34*	70.51*
	CS3	13.80	38.10	56.09*	12.70	**82.54***	**68.27***	13.80*	**38.64***	75.32*
	QDW	**13.58**	**37.71**	**54.32***	12.70	95.57*	69.76*	**13.59***	60.51*	78.34*
	QD	**13.58**	**37.71**	54.87*	12.70	–	–	13.60*	–	–
	NL	**13.58**	37.93*	54.45*	12.70	-	–	56.97*	–	–
50	CS1	26.08	86.67	150.34	29.07	202.62*	130.34*	26.07*	86.67*	133.55*
	CS2	22.83	79.60	110.36	24.84	202.62*	112.14*	22.83	79.60*	**110.35***
	CS3	21.95	77.09*	**110.36***	22.84	202.62*	**110.36***	19.97	**77.54***	110.63*
	QDW	**18.86**	**75.51***	**117.28***	**21.46**	**202.62***	**132.2***	**18.88***	86.67*	134.28*
	QD	**18.86**	**75.51***	-	**21.46**	–	–	75.17*	–	–
	NL	**18.86**	79.14*	–	36.61*	–	–	–	–	–
75	CS1	65.89	130.58	189.61	44.74	–	174.19*	39.15*	148.53*	166.48*
	CS2	31.61	130.58	168.41	35.50	–	158.94*	31.61*	144.99*	**150.67**
	CS3	31.61	**126.85***	**164.68***	34.01*	-	**157.24***	**29.19***	**143.25***	150.99*
	QDW	**28.3**	130.57*	168.75*	**32.18**	-	170.74*	53.81*	130.57*	187.86*
	QD	**28.3**	–	–	**32.18**	–	–	–	–	–
	NL	**28.3**	–	–	–	–	–	–	–	–

Bold value indicates the best possible results among all models

Asterisks (*) indicate the best found (feasible) solutions when optimality could not be proven

Table 2 Solution time (in seconds) for all structures solved by the 6 models

Structures from Fig. 2										
Load	Model	(a)	(b)	(c)	(d)	(e)	(f)	(g)	(h)	(i)
25	CS1	0.76	57.17	10.98	2.52	**TL**	**TL**	23.38	**TL**	**TL**
	CS2	1.15	65.69	444.59	4.04	**TL**	**TL**	28.13	**TL**	**TL**
	CS3	0.87	630.00	**TL**	4.88	**TL**	**TL**	62.98	**TL**	**TL**
	QDW	0.82	61.10	**TL**	18.38	**TL**	**TL**	**TL**	**TL**	**TL**
	QD	0.76	64.65	**TL**	9.49	–	–	**TL**	–	–
	NL	20.53	**TL**	**TL**	222.10	–	–	**TL**	–	–
50	CS1	1.00	24.70	41.99	78.45	**TL**	**TL**	**TL**	**TL**	**TL**
	CS2	0.91	1568.60	6043.40	100.40	**TL**	**TL**	15240.24	**TL**	**TL**
	CS3	1.54	**TL**	**TL**	120.92	**TL**	**TL**	1488.05	**TL**	**TL**
	QDW	1.28	**TL**	**TL**	404.86	**TL**	**TL**	**TL**	**TL**	**TL**
	QD	2.17	**TL**	–	368.82	–	–	**TL**	–	–
	NL	97.73	**TL**	–	**TL**	–	–	–	–	–
75	CS1	2.34	31.97	17.19	696.28	–	**TL**	**TL**	**TL**	**TL**
	CS2	1.83	3184.62	8429.44	4372.74	–	**TL**	**TL**	**TL**	**TL**
	CS3	6.55	**TL**	**TL**	**TL**	–	**TL**	**TL**	**TL**	**TL**
	QDW	1.45	**TL**	**TL**	6620.9	–	**TL**	**TL**	**TL**	**TL**
	QD	1.95	–	–	15302	–	–	–	–	–
	NL	531.47	-	–	–	–	–	–	–	–

(in advance of the optimization model formulation) without significant computational burden. Note that since the goal of our numerical experiments is to determine the scale of frame optimization problems that can be solved to optimality (and since the main conclusion is that most practical frame optimization problems remain too computationally challenging for exact global optimization models), we do not expect that the particular choice of the angle criterion will have a significant effect on the outcome, as long as it is not too restrictive, so as to still allow for some flexibility

Table 3 Optimality gap (%) for all structures solved by the 6 models

Structures from Fig. 2										
Load	Model	(a)	(b)	(c)	(d)	(e)	(f)	(g)	(h)	(i)
25	CS1	0	0	0	0	57.3	62.90	0	62.06	76.36
	CS2	0	0	0	0	64.06	62.71	0	58.34	74.06
	CS3	0	0	19.16	0	70.02	65.88	0	55.90	79.42
	QDW	0	0	13.45	0	71.68	65.55	2.81	73.83	82.52
	QD	0	0	14.32	0	–	–	3.37	–	–
	NL	0	0.01	–	0	–	–	–	–	–
50	CS1	0	0	0	0	67.65	72.41	10.02	75.34	85.73
	CS2	0	0	0	0	84.28	76.59	0	76.85	82.66
	CS3	0	28.49	53.52	0	86.93	78.56	0	76.76	84.38
	QDW	0	15.11	44.33	0	83.46	78.88	17.17	78.62	87.10
	QD	0	14.64	–	0	–	–	44.87	–	–
	NL	0	–	–	–	-	–	–	-	–
75	CS1	0	0	0	0	–	66.78	42.47	83.18	87.48
	CS2	0	0	0	0	–	80.59	39.90	85.65	86.48
	CS3	0	46.76	60.77	19.55	–	83.52	33.53	86.72	86.88
	QDW	0	37.15	48.96	0	–	80.30	66.92	83.66	89.33
	QD	0	–	–	0	–	–	–	–	–
	NL	0	–	–	–	–	–	–	–	–

in the design space. Consequently, we do not explicitly test whether the relative performance of the models is sensitive to the specific choice of the manufacturability angle (or inclusion/exclusion of horizontal elements).

Boundary conditions and external loads. We consider three pairs of boundary conditions/external loads, which in combination with the three ground structures result in the nine cases given on Fig. 2, where blue nodes represent the fixed locations (displacements set to 0), while vertical upward and downward loads are applied at the green and red nodes respectively. Unlike some existing approaches in the literature where the loads are normalized to unit, for each of the nine cases, we apply three load magnitudes: 25, 50, and 75 kN , to be able to assess the scale (and difficulty) of problems that can be solved with each solver. The values of the loads (and displacement limits) are selected so that the lowest values result in fairly simple structures with just a handful of beams, while the heaviest loads are close to the maximum feasible load for the structures given the limit on displacement and material properties. This results in a total of 27 test instances, which span from "very easy to solve " to "not being able to solve within time limit" for all models.

It is also worth noting that due to symmetry and since we keep the size of the design space constant, 3×3 structures are restrictions of the corresponding 5×5 cases, and so we expect that the latter should result in lighter weight solutions (at optimality).

Material properties. We set $E = 109$ GPa (Young's modulus of elasticity for steel) which is assumed to be fixed for all members. Displacements are limited to $[-0.095\,\text{mm}, +0.095\,\text{mm}]$ in horizontal and vertical directions. We also assume that beam elements in the structure have circular cross-sections with constant radius along the members. Without loss of generality, we set material density (ρ) to 1.

Candidate sets. All 27 instances were solved with the three exact formulations (MINLP, MIQCP with warm-start, and MIQCP without warm-start) and three versions of the MILP model with the following cross-sectional area candidate sets (in mm^2):

- $Set_1 = \{0, \pi(0.2)^2, \pi(0.5)^2\}$;
- $Set_2 = \{0, \pi(0.2)^2, \pi(0.3)^2, \pi(0.4)^2, \pi(0.5)^2\}$;
- $Set_3 = \{0, \pi(0.2)^2, \pi(0.25)^2, \pi(0.30)^2, \pi(0.35)^2, \pi(0.40)^2, \pi(0.45)^2, \pi(0.5)^2\}$.

Naturally, all three include 0 as an option to allow for excluding some of the beams, and $Set_1 \subset Set_2 \subset Set_3$. Consequently, we expect that each optimal solution to the subsequent MILP version closer approximates the continuous case. On the other hand, each results in more binary variables, and thus, is more computationally expensive. Through the rest of this section we will refer to the models as:

- NL: Mixed integer non-linear model with continuous and binary variables (Sec. 3.2);
- CS1: Linear model solved with Set_1 (Sec. 3.3);
- CS2: Linear model solved with Set_2 (Sec. 3.3);
- CS3: Linear model solved with Set_3 (Sec. 3.3);

- QDW: Mixed integer quadratically constrained model with semi-continuous variables and warm-start(Sec. 3.4).
- QD: Mixed integer quadratically constrained model with semi-continuous variables (Sec. 3.4).

In addition, note that we attempt to solve each instance and each formulation with and without the two-stage initial solution approach described above.

Implementation details and solver selection. All model construction has been implemented in Pyomo (Hart et al. 2011, 2017) and Gurobi's interface for Python (Gurobipy) (Gurobi Optimization 2021). Once modelled, all instances were solved with off-the-shelf commercial solvers, selected as described below. All experiments unless specifically mentioned were performed on a desktop computer with Intel® Core™ i7-10700K CPU @ 3.80 GHz, 64.0 GB installed memory, running on a 64-bit Windows 10 Enterprise OS with solver time limit set to 5 hours (18,000 seconds).

MINLP model is a general mixed-integer programming problem with non-convex continuous relaxation. While there exist a few available exact solvers, these can be unreliable and their relative performance is often instance-dependent. For our experiments we selected BARON (Sahinidis 2017), which is often considered as one of the best available general purpose global optimization solvers (Neumaier et al. 2005; Kronqvist et al. 2019).

MILP formulation results in a standard mixed-integer linear problem. While it is still NP-hard and computationally challenging, there exist reliable and efficient available solvers. We chose to use Gurobi for the following reasons. First, we conducted preliminary experiments with other solvers (specifically, CPLEX and Xpress) but we did not observe consistent pattern in relative performance of the linear solvers for our instances. Secondly, Gurobi is the only one that also allows for non-convex MIQP problems, and thus a direct implementation of the MIQCP model.

MIQCP formulation improves on the MINLP by only using quadratic constraints, which introduces additional structure to the problem. Note that due to this structure, we would expect this formulation to outperform the MINLP version even when used with a general global solver. Gurobi version 9.0 or newer is able to naitively solve problems with (non-convex) quadratic constraints by transforming them into bilinear constraints. These are then handled by a spacial branch-and-bound algorithm, which uses a specialized cutting plane approach. More details on the specific implementation are available in the software documentation (Gurobi Optimization 2021). In general in spatial branch and bound methods (sBB), designed for MINLPs, branching happens not only on the integer, as is the case in usual branch-and-bound algorithm, but also on the continuous variables, which allows for efficient exploration of the whole feasible set, while generating tighter relaxations. For more details of sBB method, we refer the reader to Smith and Pantelides (1999). Detailed description of other implementation techniques used in solving non-convex MIQCPs, such as valid inequalities, or relaxation tightening is beyond the scope of this paper and can be found in, for example, Castro (2015). Note that, in addition to direct support for non-convex quadratic constraints, Gurobi also allows for explicit use of semi-continuous variables, which simplifies implementation of the proposed model, and consequently, we use Gurobi for these instances.

4.2 Numerical results

In the remainder of this section, we make observations by systematically comparing all the models across all instances. In general, the resulting structures can be compared in terms of three metrics: total weight, solution time and optimality gap. In Tables 1, 2, and 3 we respectively report total weight of the resulting structures, solution times (in seconds), and the optimality gaps (in percent) when the time limit was reached by the solver. In these tables, we also note instances for which the models could not identify any feasible solution (i.e., infinite gap) labelled with a dash "-", separately from the instances where a feasible, but not provably optimal solution was found labelled with asterisk (*) in Table 1 and **TL** in Table 2. Naturally, these instances correspond to non-zero optimality gap in Table 3. In each Table, we report on the performance of six models, as discussed in detail in Sect. 4.1.

Figure 3 at the end of this section depicts the structures obtained from the linear, two-stage quadratic and nonlinear models solving the instances for ground structure given on Fig. 2d with 50 kN load. We will use it as an example illustrating our conclusions. Depictions of all solutions for each of the 27 instances and 6 models are not given in here for the sake of brevity, but can be found in the Github repository mentioned in the 'Declarations' section.

Observe that in theory, formulations MINLP and MIQCP are equivalent and hence at optimally should produce structures of the same total weight, while potentially requiring different computational effort. On the other hand, MILP is a restricted formulation, and so at optimally it should produce a structure heavier than the optimal MIQCP structure. Further, the more options for cross-sectional areas that are considered, the closer the MILP should approximate the MIQCP optimal solution. Note though that since a time limit of 5 hours was applied to all instances, these relationships may not hold for all cases in the experiments. Consequently, we choose to report the weight of the resulting structures, even when suboptimal, since, together with the corresponding gap, it enables us to make some conclusions on the performance of the three models. Observe that, overall, across all models and structures increasing external load leads to

both heavier structures and higher computational time (and optimality gap). Both observations are expected, as higher load naturally requires a sturdier structure, which in turn, can be expected to be more challenging to find.

First, let us compare the two versions of MIQCP model: with (QDW) and without (QD) warm start. Most importantly, observe that, while with the two-stage approach we are able to at least identify a feasible structure, the one-stage method cannot find any solution within the time limit in majority of cases, which can be a significant drawback in practical setting. The two stage approach also resulted in smaller optimality gap in all but one of the cases, and comparable solution time (which includes time for both stages) for instances that were able to be solved to optimality. Consequently, we conclude that the single-stage method is not competitive against QDW.

Next, compare the quadratic and nonlinear formulations. As discussed in Sect. 4.1, by introducing special problem structure, we can expect that MIQCP model should strictly outperform MINLP model even if solved by the same solver. This discrepancy should only increase, when implemented with the specialized quadratic programming rather than a general purpose global solver. We verify this conclusion with the experiments. As observed in the Tables, MIQCP outperforms MINLP model, in most cases significantly. Consequently, we conclude that the former is preferred to the latter in all cases.

Finally, compare the linear models and the quadratic approach. Consider the instances that were solved within the time limit. As we have noted earlier, the expected outcome in this case is to observe "weight of CS1" $\geq$ "weight of CS2" $\geq$ "weight of CS3" $\geq$ "weight of QDW" = "weight of NL" based on the formulation properties. This is indeed evident in Table 1 for almost all of the cases in the left half of table where the instances can be solved optimally.

It is worth emphasizing that it is impossible to evaluate in advance how far the obtained structure for the linear models (CS1–CS3) will be from the exact globally optimal solution. In our experiments, while in some cases CS1 optimal solution is close to QDW (e.g., (d) with load 25 kN), in others the quality of the CS1 solution (in terms of weight), can be extremely poor (e.g., instances (b) load 25 kN and instance (a) load 75 kN among others). We can then conclude that if an optimal solution can be expected to be obtained within the constraints of the available computational resources, QDW model can be viewed as generally outperforming the linear models, as it is expected to return lighter structures with computational effort comparable to the linear formulations with more alternatives. Consequently, we can conclude that the only reason to consider the linear version is if computational resources are severely restricted, in which case it is not advisable to consider more than 4 options (including 0) for the beam cross-sectional areas, as those are outperformed by QDW model.

Unfortunately, our experiments also demonstrate that obtaining an optimal solution found within the time limit is only possible for relatively small instances. QDW formulation was able to find the exact solution for none of the 5-by-5 instances and only the easiest of 4-by-4 ones. Note though that even comparing optimal (or lower gap) CS1–CS3 structures against suboptimal QDW solutions, we cannot conclusively declare that either approach consistently produces lighter structures. Indeed, each of the models (CS1–CS3, QDW) produced the best structure within the time limit for at least one ground structure and load combination. Consequently, even when QDW model does not find the global optimum within the time limit, it is still competitive with the linear formulations, though all finish with relatively large optimality gaps (up to 89%) in some cases.

5 Conclusions

In this paper, we modeled and solved the topology optimization problem of designing minimum-weight planar frame structures for additive manufacturing using three different mathematical modeling approaches. While recent advances in exact optimization software and available computing resources suggest a potential wider applicability of exact methods in solving these challenging problems, unfortunately, our experiments demonstrate that it is still only possible for relatively small instances. Consequently, we characterize the extent to which exact global optimization is possible in AM setting.

The first contribution of this work is in incorporating AM manufacturability constraints into the existing models for the frame structure optimization problem. Second, we build on two existing approaches in the literature to propose a new model that is designed to take advantage of progress in global optimization software. The traditional modeling approach includes nonlinearity in the equilibrium equations, resulting in a Mixed-Integer Nonlinear Programming formulation with non-convex continuous relaxation. A linearized formulation can be obtained by assuming a discrete set of beam diameters and using a decomposition of the stiffness matrix. As a way to address the computational challenges inherent to both existing formulations we propose a Mixed-Integer Quadratically-Constrained Programming formulation of the problem by employing semi-continuous variables.

We compare the results of these models in terms of structures' weight and the solving time. All three formulations can be solved with off-the-shelf commercial solvers. Note though that each poses significant computational challenges. Specifically, MINLP formulation is explicitly non-convex, and while there exist general-purpose global optimization

tools (e.g., BARON, used in our experiments), they are still rather limited in their ability to solve practical problems in the absence of some particular problem structure. MIQCP formulation partially alleviates this issue by relying on quadratic constraints only, and hence is able to take advantage of more specialized software. At the same time, the formulation is still non-convex and so is still hard to solve. The three models were implemented to solve frame optimization instances with various test ground structures.

First, our results show that the proposed quadratic model easily out-performs the MINLP model in all cases. We also note that the quadratic model together with the proposed two-stage approach to solve the experimental instances can find at least a feasible solution for 26 out of 27 structure/load combinations. The two-stage approach helps solving the problem in two directions: (1) infeasibility of the first stage proves the infeasibility of the instance; (2) at least a feasible solution can be found for all of the instances for which the first stage resulted in a solution. Consequently, we conclude that as far as exact mathematical programming formulations are concerned, MIQCP version with two-stage solution approach is superior.

The linear formulation can rely on efficient modern MILP solvers (CPLEX, Gurobi, etc), which are generally more reliable and efficient than the non-linear counterparts. At the same time, by design, it is a restricted formulation, meaning that it cannot be guaranteed to find the exact optimal solution or in general provide a tight bound on how far the identified approximate solution is from the global optimum. Second, to eliminate non-convexity it introduces a large number of binary variables, especially if more than a handful of profile options are considered. Consequently, the linear model may still be hard to solve and may result in inferior optimal solutions. Our experiments indicate that, in general, linear formulation can only be recommended if few (up to 3-4) options for dimensions per beam are considered. In those cases, the formulation can be expected to find a solution faster than the exact MIQCP, assuming that exact global optimum is not important. On the other hand, MIQCP generally outperforms or is comparable with larger linear formulations.

It must be emphasized that despite the progress in both hardware and off-the-shelf optimization software, even the best models considered here for discrete topology optimization of frames are still restricted in terms of the scale of problems solved. On one hand, the MIQCP model performs best in the easiest instances and its performance is comparable with a linear model (with a modest set of available cross-sectional areas) for the larger ones tested. On the other hand, all the instances included in this study are smaller than a typical practical problem. Hence, this study has also shown that pure mathematical programming approaches are not well suited for real-world applications of this problem.

It is also worth noting that while hardware improvements (or extended time limits) might somewhat increase the scale of instances that can be solved to global optimality, our experience with these and similar problems suggests that only very modest increase can actually be expected. Indeed, observe that in our case study almost none of the 5×5 instances can achieve optimality gap below 50%. In difficult (non-convex, mixed-integer) optimization problems, it is usually much easier to find a relatively good solution, than it is to actually close the optimality gap (or prove its optimality). Consequently, given the size of the observed gap, we do not expect that any of the considered methods would be able to find global optimum on the same hardware within any reasonable time limit for any of the hardest 5×5 instances. It may be an interesting research question to consider the extent to which a supercomputer might be able to speed up the procedure, but even then our experience suggests that exact global optima for any practical frame optimization problems remain unattainable.

Future work should consider heuristic or metaheuristic methods to quickly find good (albeit sub-optimal) solutions to realistically sized problems. Note that the MIQCP model proposed here can still be relevant for such efforts. First, a continuous relaxation (or restriction based on particular binary variables' values) can serve as a subroutine in a heuristic approach. For example, if binary variables are fixed (i.e., if beams present in the structure are preselected), beam-sizing problem should still be solved by employing the quadratic version of the equilibrium constraint as opposed to the general non-linear one. Further, our methodology can be useful for validating any possible heuristic methods, at least for smaller instances.

Appendix

Using the relations between displacement and external nodal loads from matrix analysis of the frame structures, we can define the stiffness matrix of each beam element in its local coordinate system as follow:

$$\mathbf{k}_e(a_e, I_e) = \begin{pmatrix} \frac{a_e E}{l_e} & 0 & 0 & -\frac{a_e E}{l_e} & 0 & 0 \\ 0 & \frac{12 I_e E}{l_e^3} & \frac{6 I_e E}{l_e^2} & 0 & -\frac{12 I_e E}{l_e^3} & \frac{6 I_e E}{l_e^2} \\ 0 & \frac{6 I_e E}{l_e^2} & \frac{4 I_e E}{l_e} & 0 & -\frac{6 I_e E}{l_e^2} & \frac{2 I_e E}{l_e} \\ -\frac{a_e E}{l_e} & 0 & 0 & \frac{a_e E}{l_e} & 0 & 0 \\ 0 & -\frac{12 I_e E}{l_e^3} & -\frac{6 I_e E}{l_e^2} & 0 & \frac{12 I_e E}{l_e^3} & -\frac{6 I_e E}{l_e^2} \\ 0 & \frac{6 I_e E}{l_e^2} & \frac{2 I_e E}{l_e} & 0 & -\frac{6 I_e E}{l_e^2} & \frac{4 I_e E}{l_e} \end{pmatrix} \tag{A.1}$$

$\mathbf{k}_e \in \mathbb{R}^{6\times 6}$ is a symmetric positive definite matrix in which, a_e and I_e represents the two cross-sectional properties, namely area and moment of inertia, of the element e (Kassimali (2012)). In order to reduce the number of decision variables in our mathematical models, we can relate the moment of inertia for circular beams to their cross-sectional area as follows (r_e is the radius of element e):

$$I_e = \frac{\pi r_e^4}{4} = \frac{a_e^2}{4\pi} \tag{A.2}$$

Equilibrium state of the structure, where the internal forces and external nodal loads are balancing each other, can be illustrated in the model by using equilibrium equations:

$$\mathbf{K}(\mathbf{a}, \mathbf{I})\mathbf{u} = \mathbf{P} \tag{A.3}$$

Equation (A.3) represents d similar constraints in the mathematical model. In (A.3), $\mathbf{K} \in \mathbb{R}^{d\times d}$ is the global stiffness matrix of the structure. $\mathbf{u}$ and $\mathbf{P}$ are $d \times 1$ vectors representing respectively, displacements and the external nodal loads on all degrees of freedom. Although we will explain it later in detail, it should be noted here that $\mathbf{K}$ is constructed using the members' stiffness matrices in a global coordinate system. Based on the boundary conditions, for some of the degrees of freedom j, $u_j = 0$ and for some degrees of freedom j, p_j is a variable representing reaction forces on the fixed nodes. Based on the mentioned boundary condition effects, we express each equation of (A.3) in the form of the constraints in mathematical models as follow:

$$\sum_{j=1}^{d} \mathbf{K}_{ij} u_j = p_i \qquad \forall i \in \mathbb{S}_{\text{dof}} \tag{A.4}$$

We assume that external loads exist only on the end-nodes of the elements not along them. Loads also assumed to be concentrated dead loads which means they are deterministic,given, and do not change during the analysis. $\mathbf{k}_e$ in (A.1), and as a consequence, $\mathbf{K}$ in (A.3), include a_e and I_e which are decision variables in the model. In finite element analysis, to avoid matrix inversion in solving the system of equations in (A.3), usually different decomposition methods such as LU decomposition, Cholesky decomposition, or Singular Value Decomposition are used. Here, following the approach that (Stolpe and Svanberg 2003; Stolpe 2004; Rasmussen and Stolpe 2008; Kanno 2016) suggested, we decompose the stiffness matrices in (A.1). We define the following vectors together with the eigenvalues:

$$\hat{\mathbf{b}_{\mathbf{e1}}} = \begin{pmatrix} -1 \\ 0 \\ 0 \\ 1 \\ 0 \\ 0 \end{pmatrix}, \quad \hat{\mathbf{b}_{\mathbf{e2}}} = \begin{pmatrix} 0 \\ 2/l_e \\ 1 \\ 0 \\ -2/l_e \\ 1 \end{pmatrix}, \quad \hat{\mathbf{b}_{\mathbf{e3}}} = \begin{pmatrix} 0 \\ 0 \\ -1 \\ 0 \\ 0 \\ 1 \end{pmatrix} \quad \forall e \in \mathbb{S}_e \tag{A.5}$$

$$k_{e1} = \frac{a_e E}{l_e}, \quad k_{e2} = \frac{3 I_e E}{l_e}, \; k_{e3} = \frac{I_e E}{l_e} \tag{A.6}$$

The member stiffness matrix in local coordinates can be obtained using the following matrix multiplication:

$$\mathbf{k}_e = \sum_{z=1}^{3} k_{ez} \hat{\boldsymbol{b}}_{ez} (\hat{\boldsymbol{b}}_{ez}^{\mathsf{T}}) \tag{A.7}$$

where $\hat{\boldsymbol{b}}_{ez}(\hat{\boldsymbol{b}}_{ez}^{\mathsf{T}})$ represents the outer product of the two vectors $\hat{\boldsymbol{b}}_{ez} \in \mathbb{R}^{6\times 1}$ and $\hat{\boldsymbol{b}}_{ez}^{\mathsf{T}} \in \mathbb{R}^{1\times 6}$, which results in a matrix in $\mathbb{R}^{6\times 6}$. Using Eq. (A.2) we can replace I_e with $a_e^2/4\pi$ and rewrite the decomposition in (A.7) as:

$$\mathbf{k}_e = \frac{a_e E}{l_e} \hat{\boldsymbol{b}}_{\boldsymbol{e1}} (\hat{\boldsymbol{b}}_{\boldsymbol{e1}}^{\mathsf{T}}) + \frac{3 a_e^2 E}{4\pi l_e} \hat{\boldsymbol{b}}_{\boldsymbol{e2}} (\hat{\boldsymbol{b}}_{\boldsymbol{e2}}^{\mathsf{T}}) + \frac{a_e^2 E}{4\pi l_e} \hat{\boldsymbol{b}}_{\boldsymbol{e3}} (\hat{\boldsymbol{b}}_{\boldsymbol{e3}}^{\mathsf{T}}) \tag{A.8}$$

To be used in the construction of the structure's stiffness matrix, vectors in (A.5) need to be transformed to global coordinates. Considering the geometry of each beam element, we define the following transformation matrices:

$$\mathbf{Trans}_e = \begin{pmatrix} c & s & 0 & 0 & 0 & 0 \\ -s & c & 0 & 0 & 0 & 0 \\ 0 & 0 & 1 & 0 & 0 & 0 \\ 0 & 0 & 0 & c & s & 0 \\ 0 & 0 & 0 & -s & c & 0 \\ 0 & 0 & 0 & 0 & 0 & 1 \end{pmatrix}_{6\times 6}$$

In which $c = cos(\theta_e)$, $s = sin(\theta_e)$. To assemble the global stiffness matrix of the structure, we define the element specified $\mathbf{T}_e \in \mathbb{R}^{6\times d}$ matrices. Each $\mathbf{T}_e$ is a $6 \times d$ binary location matrix that relates the element's degrees of freedom to the degrees of freedom in the structure. Consider element e which connects node 2 (degrees of freedom: $\{4, 5, 6\}$) and node 4 (degrees of freedom: $\{10, 11, 12\}$), the degrees of freedom of element e are: $\{4, 5, 6, 10, 11, 12\}$ and the $\mathbf{T}_e$ matrix for this element can be defined as:

$$\mathbf{T}_3 = \begin{array}{c} \begin{matrix} 1 & 2 & 3 & 4 & 5 & 6 & 7 & 8 & 9 & 10 & 11 & 12 & 13 & 14 & \dots & d \end{matrix} \\ \begin{pmatrix} 0 & 0 & 0 & 1 & 0 & 0 & 0 & 0 & 0 & 0 & 0 & 0 & 0 & 0 & \dots & 0 \\ 0 & 0 & 0 & 0 & 1 & 0 & 0 & 0 & 0 & 0 & 0 & 0 & 0 & 0 & \dots & 0 \\ 0 & 0 & 0 & 0 & 0 & 1 & 0 & 0 & 0 & 0 & 0 & 0 & 0 & 0 & \dots & 0 \\ 0 & 0 & 0 & 0 & 0 & 0 & 0 & 0 & 0 & 1 & 0 & 0 & 0 & 0 & \dots & 0 \\ 0 & 0 & 0 & 0 & 0 & 0 & 0 & 0 & 0 & 0 & 1 & 0 & 0 & 0 & \dots & 0 \\ 0 & 0 & 0 & 0 & 0 & 0 & 0 & 0 & 0 & 0 & 0 & 1 & 0 & 0 & \dots & 0 \end{pmatrix}_{6\times d} \end{array}$$

The following transformation of the $\hat{\boldsymbol{b}}_{\boldsymbol{e}}$ matrices are used in the generating of equilibrium equations:

$$\mathbf{b_e} = \mathbf{T}_e^{\mathsf{T}} \times \mathbf{Trans}_e^{\mathsf{T}} \times \hat{\boldsymbol{b}}_{\boldsymbol{e}} \tag{A.9}$$

for which as mentioned before, $\mathbf{T}_e^{\mathsf{T}} \in \mathbb{R}^{d\times 6}$, $\mathbf{Trans}_e^{\mathsf{T}} \in \mathbb{R}^{6\times 6}$, and $\hat{\boldsymbol{b}}_{\boldsymbol{e}} \in \mathbb{R}^{6\times 1}$, therefore $\mathbf{b_e} \in \mathbb{R}^{d\times 1}$. Using these equations and values in (3.2), equation (A.4) can be written as (notice that $\mathbf{b_{e1}} \wedge \mathbf{b_{e1}^{\mathsf{T}}}$ and $\mathbf{b_{e2}} \wedge \mathbf{b_{e2}^{\mathsf{T}}}$ and $\mathbf{b_{e3}} \wedge \mathbf{b_{e3}^{\mathsf{T}}} \in \mathbb{R}^{d\times d}$):

$$\left(\sum_{e\in\mathbb{S}_e} k_{e1} \mathbf{b_{e1}} (\mathbf{b_{e1}^{\mathsf{T}}}) + k_{e2} \mathbf{b_{e2}} (\mathbf{b_{e2}^{\mathsf{T}}}) + k_{e3} \mathbf{b_{e3}} (\mathbf{b_{e3}^{\mathsf{T}}}) \right)_i \mathbf{u} = p_i \;\; \forall i \in \mathbb{S}_{\text{dof}} \tag{A.10}$$

In the above equation, the summation is the global stiffness matrix of the structure that was generated using the relations (A.5) through (A.9).

Declarations

Conflict of interest The authors declare that they have no conflict of interest.

Replication of results To facilitate the replication of our results, we have shared all Pyomo, Gurobipy, and Python codes for all models as well as the ground structure generation codes in the first author's Github account https://github.com/oguztoragay/AMmodels.

References

Achtziger W, Stolpe M (2007) Truss topology optimization with discrete design variables–guaranteed global optimality and benchmark examples. Struct Multidisc Optim 34(1):1–20

Bendsoe MP, Sigmund O (2013) Topology optimization: theory, methods, and applications. Springer Science & Business Media, Berlin

Bollapragada S, Ghattas O, Hooker JN (2001) Optimal design of truss structures by logic-based branch and cut. Oper Res 49(1):42–51

Cansizoglu O, Harrysson OL, West HA, Cormier DR, Mahale T (2008) Applications of structural optimization in direct metal fabrication. Rapid Prototyp J

Castro PM (2015) Tightening piecewise mccormick relaxations for bilinear problems. Comput Chem Eng 72:300–311

Cerveira A, Agra A, Bastos F, Gromicho J (2013) A new branch and bound method for a discrete truss topology design problem. Comput Optim Appl 54(1):163–187

Chan CM (1992) An optimality criteria algorithm for tall steel building design using commercial standard sections. Struct Optim 5(1–2):26–29

Changizi N, Jalalpour M (2017a) Robust topology optimization of frame structures under geometric or material properties uncertainties. Struct Multidisc Optim 56(4):791–807

Changizi N, Jalalpour M (2017b) Stress-based topology optimization of steel-frame structures using members with standard cross sections: Gradient-based approach. J Struct Eng 143(8):04017078

Cui H, An H, Huang H (2018) Truss topology optimization considering local buckling constraints and restrictions on intersection and overlap of bar members. Struct Multidisc Optim 58(2):575–594

Deaton JD, Grandhi RV (2014) A survey of structural and multidisciplinary continuum topology optimization: post 2000. Struct Multidisc Optim 49(1):1–38

Dorn W (1964) Automatic design of optimal structures. J de Mec 3:25–52

Erbatur F, Hasançebi O, Tütüncü I, Kılıç H (2000) Optimal design of planar and space structures with genetic algorithms. Comput Struct 75(2):209–224

Eschenauer HA, Olhoff N (2001) Topology optimization of continuum structures: a review. Appl Mech Rev 54(4):331–390

Gorguluarslan RM, Gandhi UN, Song Y, Choi SK (2017) An improved lattice structure design optimization framework considering additive manufacturing constraints. Rapid Prototyp J

Grossmann I, Voudouris V, Ghattas O (2014) Mixed-integer linear programming reformulations for some nonlinear discrete design optimization problems. Princeton University Press, Princeton, pp 478–512. https://doi.org/10.1515/9781400862528.478

Gurobi Optimization L (2021) Gurobi optimizer reference manual. http://www.gurobi.com

Hart WE, Watson JP, Woodruff DL (2011) Pyomo: modeling and solving mathematical programs in python. Math Programm Comput 3(3):219–260

Hart WE, Laird CD, Watson JP, Woodruff DL, Hackebeil GA, Nicholson BL, Siirola JD (2017) Pyomo-optimization modeling in python, vol 67, 2nd edn. Springer Science & Business Media, Berlin

Hayashi K, Ohsaki M (2020) Reinforcement learning for optimum design of a plane frame under static loads. Eng Comput. https://doi.org/10.1007/s00366-019-00926-7

Kanno Y (2016) Mixed-integer second-order cone programming for global optimization of compliance of frame structure with discrete design variables. Struct Multidisc Optim 54(2):301–316

Kassimali A (2012) Matrix analysis of structures SI version. Cengage Learning, Boston

Kaveh A, Zolghadr A (2014) Comparison of nine meta-heuristic algorithms for optimal design of truss structures with frequency constraints. Adv Eng Softw 76:9–30

Klanšek U, Žula T, Kravanja Z, Kravanja S (2007) Minlp optimization of steel frames. Adv Steel Constr 3(3):689–705

Kočvara M, Outrata JV (2006) Effective reformulations of the truss topology design problem. Optim Eng 7(2):201–219

Kronqvist J, Bernal DE, Lundell A, Grossmann IE (2019) A review and comparison of solvers for convex minlp. Optimiz Eng 20(2):397–455

Kureta R, Kanno Y (2014) A mixed integer programming approach to designing periodic frame structures with negative poisson's ratio. Optim Eng 15(3):773–800

Li Y, Chen Y (2010) Beam structure optimization for additive manufacturing based on principal stress lines. In: Solid freeform fabrication proceedings, pp 666–678

Liu J, Ma Y (2016) A survey of manufacturing oriented topology optimization methods. Adv Eng Softw 100:161–175

Liu J, Yu H (2020) Self-support topology optimization with horizontal overhangs for additive manufacturing. J Manuf Sci Eng 142(9):091003

Lobo MS, Vandenberghe L, Boyd S, Lebret H (1998) Applications of second-order cone programming. Linear Algebra Its Appl 284(1–3):193–228

Makrodimopoulos A, Bhaskar A, Keane AJ (2010) Second-order cone programming formulations for a class of problems in structural optimization. Struct Multidisc Optim 40(1–6):365

Michell AGM (1904) Lviii. the limits of economy of material in frame-structures. J Sci 8(47):589–597

Neumaier A, Shcherbina O, Huyer W, Vinkó T (2005) A comparison of complete global optimization solvers. Math Programm 103(2):335–356

Querin OM, Victoria M, Gordoa CA, Ansola R, Martí P (2017) Topology design methods for structural optimization. Butterworth-Heinemann, Oxford

Rasmussen M, Stolpe M (2008) Global optimization of discrete truss topology design problems using a parallel cut-and-branch method. Comput Struct 86(13–14):1527–1538

Sahinidis NV (2017) BARON 21.1.13: global optimization of mixed-integer nonlinear programs. User's manual

Saka MP, Geem ZW (2013) Mathematical and metaheuristic applications in design optimization of steel frame structures: an extensive review. Math Prob Eng. https://doi.org/10.1155/2013/271031

Smith CJ, Gilbert M, Todd I, Derguti F (2016) Application of layout optimization to the design of additively manufactured metallic components. Struct Multidisc Optim 54(5):1297–1313

Smith EM, Pantelides CC (1999) A symbolic reformulation/spatial branch-and-bound algorithm for the global optimisation of nonconvex minlps. Comput Chem Eng 23(4–5):457–478

Stolpe M (2004) Global optimization of minimum weight truss topology problems with stress, displacement, and local buckling constraints using branch-and-bound. Int J Numer Methods Eng 61(8):1270–1309

Stolpe M (2007) On the reformulation of topology optimization problems as linear or convex quadratic mixed 0–1 programs. Optim Eng 8(2):163–192

Stolpe M (2016) Truss optimization with discrete design variables: a critical review. Struct Multidisc Optim 53(2):349–374

Stolpe M, Svanberg K (2003) Modelling topology optimization problems as linear mixed 0–1 programs. Int J Numer Methods Eng 57(5):723–739

Takezawa A, Nishiwaki S, Izui K, Yoshimura M (2007) Structural optimization based on topology optimization techniques using frame elements considering cross-sectional properties. Struct Multidisc Optim 34(1):41–60

Wang C, Qian X, Gerstler WD, Shubrooks J (2019) Boundary slope control in topology optimization for additive manufacturing: for self-support and surface roughness. J Manuf Sci Eng 141(9):091001

Wang D, Yang Y, Yi Z, Su X (2013) Research on the fabricating quality optimization of the overhanging surface in slm process. Int J Adv Manuf Technol 65(9–12):1471–1484

Wang X, Xu S, Zhou S, Xu W, Leary M, Choong P, Qian M, Brandt M, Xie YM (2016) Topological design and additive manufacturing of porous metals for bone scaffolds and orthopaedic implants: a review. Biomaterials 83:127–141